LA-UR- 08-2069

Approved for public release; distribution is unlimited.

Title:	Measurement of the solar neutrino capture rate with gallium metal, Part III
Author(s):	J.N. Abdurashitov, and others
Submitted to:	Physical Review C

Form 836 (8/00)

Measurement of the solar neutrino capture rate with gallium metal, Part III

J. N. Abdurashitov, V. N. Gavrin, V. V. Gorbachev, P. P. Gurkina, T. V. Ibragimova, A. V. Kalikhov, N. G. Khairnasov, T. V. Knodel, I. N. Mirmov, A. A. Shikhin, E. P. Veretenkin, V. E. Yants, and G. T. Zatsepin
Institute for Nuclear Research, Russian Academy of Sciences, 117312 Moscow, Russia

T. J. Bowles, S. R. Elliott, and W. A. Teasdale
Los Alamos National Laboratory, Los Alamos, New Mexico 87545, USA

J. S. Nico
National Institute of Standards and Technology, Stop 8461, Gaithersburg, Maryland 20899, USA

B. T. Cleveland* and J. F. Wilkerson
University of Washington, Seattle, Washington 98195, USA

(The SAGE Collaboration)
(Dated: 25 October 2008)

The Russian-American experiment SAGE began to measure the solar neutrino capture rate with a target of gallium metal in December 1989. Measurements have continued with only a few brief interruptions since that time. In this article we present the experimental improvements in SAGE since its last published data summary in December 2001. Assuming the solar neutrino production rate was constant during the period of data collection, combined analysis of 168 extractions through December 2007 gives a capture rate of solar neutrinos with energy more than 233 keV of $65.4^{+3.1}_{-3.0}$ (stat) $^{+2.6}_{-2.8}$ (syst) SNU. The weighted average of the results of all three Ga solar neutrino experiments, SAGE, Gallex, and GNO, is now 66.1 ± 3.1 SNU, where statistical and systematic uncertainties have been combined in quadrature.

During the recent period of data collection a new test of SAGE was made with a reactor-produced ^{37}Ar neutrino source. The ratio of observed to calculated rates in this experiment, combined with the measured rates in the three prior ^{51}Cr neutrino-source experiments with Ga, is 0.88 ± 0.05. A probable explanation for this low result is that the cross section for neutrino capture by the two lowest-lying excited states in ^{71}Ge has been overestimated. If we assume these cross sections are zero, then the standard solar model including neutrino oscillations predicts a total capture rate in Ga in the range of 63–67 SNU with an uncertainty of about 5%, in good agreement with experiment. We derive the current value of the *pp* neutrino flux produced in the Sun to be $\phi^{\odot}_{pp} = (6.1 \pm 0.8) \times 10^{10}/(\mathrm{cm}^2\ \mathrm{s})$, which agrees well with the flux predicted by the standard solar model. Finally, we make several tests and show that the data are consistent with the assumption that the solar neutrino production rate is constant in time.

PACS numbers: 26.65.+t, 96.60.-j, 95.85.Ry, 13.15.+g

I. INTRODUCTION

The SAGE experiment was built to measure the capture rate of solar neutrinos by the reaction $^{71}\mathrm{Ga} + \nu_e \rightarrow {}^{71}\mathrm{Ge} + e^-$ and thus to provide information to aid in understanding the deficit of neutrinos observed in the ^{37}Cl experiment [1], in which only about one-third of the solar neutrino capture rate predicted by the standard solar model was detected. The feature that distinguishes the Ga experiment from all other past or present solar neutrino detectors is its sensitivity to the proton-proton fusion reaction, $p + p \rightarrow d + e^+ + \nu_e$, which generates most of the Sun's energy. Ga experiments have provided the only direct measurement of the current rate of this reaction.

A full description of the SAGE experiment and the results of each measurement from its inception to December 1997 was presented in [2]. The next article in this series, although not called by this name, described the changes to the experiment and gave the results for the period January 1998 to December 2001 [3]. In Sections II and III of this article we do the same for the six-year period January 2002 to December 2007. We then discuss the four neutrino source experiments with Ga in Section IV, give the present interpretation of the SAGE results in Section V, derive the *contemporary* value of the *pp* flux from the Sun in Section VI, and present a brief consideration of the question of possible time variation in the data in Section VII.

In addition to SAGE, there also existed a second Ga solar neutrino experiment called Gallex. It contained 30 tons of gallium in a solution of $GaCl_3$ and measured the solar neutrino capture rate from 1991 to 1997. In 1998 this experiment was reconstituted under the name of GNO and it took data until 2003. We give the results of these experiments and combine them with the SAGE data in Section III.

*Corresponding author. Present address: SNOLAB, PO Box 159, Lively, Ontario P3Y 1M3, Canada; bclevela@snolab.ca.

II. EXPERIMENTAL PROCEDURES

A. Overview

The SAGE experiment is in a dedicated deep-underground laboratory excavated into the side of Mt. Andyrchi in the northern Caucasus mountains of Russia. The rock overburden is equivalent to 4700 m of water and the measured muon flux at the location of the experiment is $(3.03\pm0.10)\times10^{-9}/(\mathrm{cm}^2\ \mathrm{s})$.

The mass of gallium used in SAGE at the present time is 50 tonnes. It is contained in 7 chemical reactors which are heated to 30 °C so the gallium metal remains molten. A measurement of the solar neutrino capture rate begins by adding to the gallium a stable Ge carrier. The carrier is a Ga-Ge alloy with a known Ge content of approximately 350 μg and is distributed equally among all reactors. The reactor contents are stirred thoroughly to disperse the Ge throughout the Ga mass. After a typical exposure interval of one month, the Ge carrier and ^{71}Ge atoms produced by solar neutrinos and background sources are chemically extracted from the Ga. The final step of the chemical procedure is the synthesis of germane (GeH_4), which is used as a proportional counter fill gas with an admixture of (90–95)% Xe. The total efficiency of extraction is the ratio of mass of Ge in the germane to the mass of initial Ge carrier and is typically (95 ± 3)%.

B. Extraction of Ge from Ga

The extraction procedures from 1990–1997 are described in [2]. At the beginning of 1998 some minor modifications were made as described in [4].

Beginning with the December 2005 extraction, the carrier used to measure the extraction efficiency was isotopically enriched in either ^{72}Ge or ^{76}Ge. At the end of each extraction a sample was taken from the final extraction solution and this sample was analyzed with an inductively-coupled plasma mass spectrometer to determine the fractional content of the various Ge isotopes. The efficiency of Ge extraction from the Ga metal was then calculated using the method outlined in Appendix A.

C. Counting of ^{71}Ge

^{71}Ge decays back to ^{71}Ga by pure electron capture with a half life of 11.4 days. Two peaks are observed in the proportional counter – the K peak at 10.4 keV and the L peak at 1.2 keV. The counter containing the GeH_4 from the extraction is placed in the well of a NaI detector that is within a large passive shield and is counted for a typical period of 6 months. To reduce the influence of ^{222}Rn, the volume inside the shield around the counters is purged with boiloff gas from a dewar filled with liquid nitrogen.

A completely redesigned proportional counter [5] began to be used with the extraction of April 2001, and has been used for all but two extractions since that time. In contrast to the usual counters with a solid cathode, the cathode of the new counters is made from vapor-deposited carbon, thus eliminating the usual dead volume behind the cathode. The dead volume is further reduced and end effects are nearly eliminated by curving inwards the regions of the counter where the cathode ends. The cathode and anode leads are sealed into the counter body with Mo ribbon which makes the counter leak free and ensures excellent gain stability. The cathode is so thin that the counter body is transparent, making it possible to visually inspect all the internal counter parts.

During 2004–2005 an extensive series of measurements of the efficiency of these new counters was made. The methods of measurement were described in [2] and counter fillings of ^{69}Ge, ^{71}Ge, and ^{37}Ar were used. The measured volume efficiency of the new counters was 96% with a spread in efficiency of only ±1% for all counters of this type. This should be compared with an average volume efficiency of 89% for our original counter design. Further, the fraction of events that is degraded in energy was found to be significantly less than in the old design. These decreases in degraded fraction combined with the increase in volume efficiency lead to a quite dramatic increase in efficiency for these new counters compared to the old type, approximately 25% in the K peak and 10% in the L peak.

Another innovation in the new counter design is that the Suprasil counter body is etched in hydrofluoric acid to a thickness of ~0.2 mm. This permits calibration of the counter with our standard ^{55}Fe source over nearly its entire volume. As an undesired side effect, however, the thin body, combined with the very thin cathode, makes these counters sensitive to low-energy x rays from local radioactivity. To eliminate this response, a graded shield consisting of an outer layer of 1 mm of Cu and an inner layer of 3 mm of low-background acrylic (to absorb Cu x rays) is placed over the counter body during measurement with $^{71}GeH_4$.

The pulses from the proportional counter are sent to a fast transient analyzer where they are digitized for 800 ns after pulse onset at two different gains, one chosen for the L peak and the other for the K peak. The transient digitizer serves to differentiate fast-rising ^{71}Ge pulses from generally slower-rising background pulses. This can be seen by comparing the upper and lower panels of Figure 1, which show the pulses from the 77 extractions that have been measured in the new proportional counters. The upper panel is for all events that pass the time cuts for Rn (see Section II D), are not high-voltage breakdown, do not have a NaI coincidence, and occur during the first 30 days of counting. The total live time is 1999.8 days and there are 2063 events. The lower panel of this figure shows the 1545 events that occurred between days 100.0–130.1 (the same live time duration as in the upper panel). The fast-rising ^{71}Ge events in the L and K peaks are evident in the upper panel but missing in the lower panel because the ^{71}Ge has decayed away.

Aside from replacing some modules that failed, no changes were made to the counting system electronics since their description in [2].

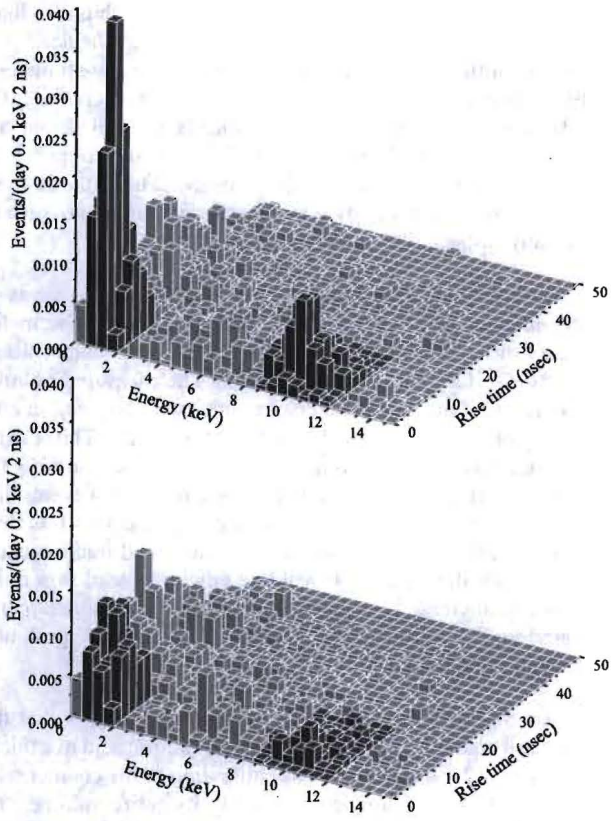

FIG. 1: Upper panel: count rate vs energy and rise time for events during the first 30 days of counting. Regions where the L and K peaks are predicted to occur based on ^{55}Fe calibrations are shown darkened. There are 427 counts in the L peak and 287 counts in the K peak. Lower panel: equivalent graph for all events that occurred during an equal live time interval beginning at day 100 after extraction. There are 226 counts in the L peak and 94 counts in the K peak.

D. Data analysis

Based on criteria described in [2], a group of events is selected from each extraction that are candidate ^{71}Ge decays. These events are fit to a maximum likelihood function [6], assuming that they originate from an unknown but constant-rate background and the exponentially-decaying rate of ^{71}Ge. Since only a few ^{71}Ge counts are detected from each extraction, a single run result has a large statistical uncertainty and thus little significance.

Several minor changes in the methods of analysis have occurred since Part II of this series. These include

- As discussed in [2], a small fraction of the decays of ^{222}Rn are occasionally mis-identified as pulses from ^{71}Ge. To reduce this effect for ^{222}Rn located external to the counter we now delete all data that is acquired within 2.6 hours after counting begins. In our initial analysis this time cut was for only one hour.

- To reduce the influence of ^{222}Rn that may enter the counter when it is filled, we delete all data from 15 min before an event that saturates the energy scale to 3 h after each saturated event. The SAGE measurements before September 1992, however, were measured in counting systems that did not have the capability to recognize saturated events. To reduce the number of these false ^{71}Ge events produced by ^{222}Rn in these early runs we determine for all subsequent runs the difference in capture rate in the K peak between the data analyzed with and without this time cut and then subtract this difference from the result of each of the runs before September 1992.

- The predicted position and resolution of the L peak from calibrations was changed slightly from previous work. These changes were indicated by the results of a set of new calibrations made with counters filled with ^{71}Ge.

- The L- and K-peak shapes were changed from pure Gaussian to Gaussian plus a degraded term. The new functional form for the line shape as a function of energy is

$$F(E) = he^{-[(E-C)/(\sqrt{2}\sigma)]^2} + hd\sqrt{\frac{\pi}{2}}\frac{\sigma}{C}\mathrm{erfc}\left(\frac{E-C}{\sqrt{2}\sigma}\right)$$

  where h, C, and σ are the peak height, center, and width and d is a parameter related to the fraction of degraded events. The error function term here is the integral of the Gaussian from energy E to ∞; it is essentially flat below the peak, monotonically decreases in the peak region, and is zero above the peak. This new line shape only makes a very small change to the counting efficiency in the L peak for a few runs whose energy window width is obliged to be less than 2 full widths at half maximum.

- For all runs after August 1992 the likelihood function was modified to include a factor that weights each event according to its measured energy. This requires knowledge of the energy distribution for ^{71}Ge pulses and for background events, both of which can be determined from the long duration of counting data that we have accumulated. When this method is applied, it is found that the overall statistical error decreases by (0.1-0.2) SNU, but the systematic error increases by ~0.1 SNU.

These changes in analysis methods have been applied to all data.

III. RESULTS

^{71}Ge has been extracted from the Ga target to measure the solar neutrino capture rate every month from January 2000 to the present time. We even were able to make six solar extractions during the time of the ^{37}Ar neutrino source experiment

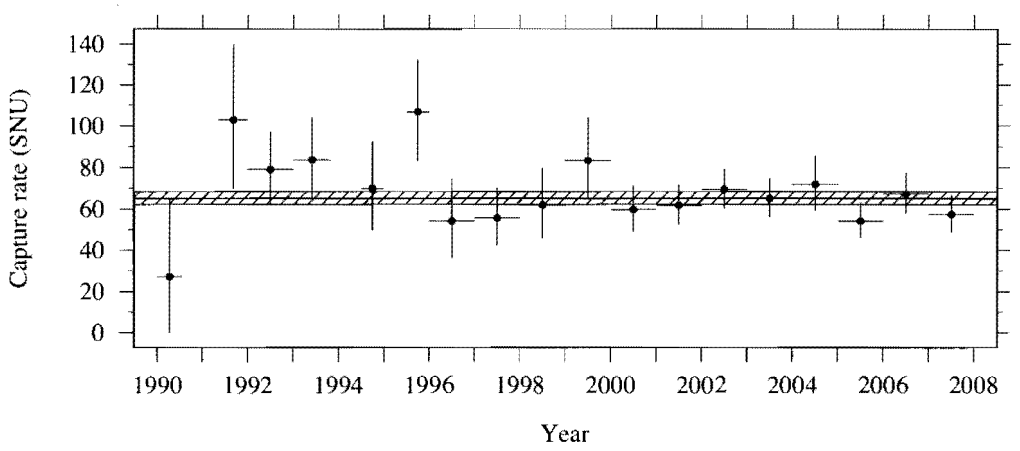

FIG. 2: Combined SAGE results for each year. Shaded band is the combined best fit and its uncertainty for all years. Vertical error bars are statistical with 68% confidence.

TABLE I: Summary of systematic effects and their uncertainties. SNU values for extraction and counting efficiency are based on a rate of 65.4 SNU.

	Uncertainty	
Origin of uncertainty	in percent	in SNU
Extraction efficiency		
Ge carrier mass	±2.1%	±1.4
Mass of extracted Ge	±2.5%	±1.6
Residual Ge carrier	±0.8%	±0.5
Ga mass	±0.3%	±0.2
Total (extraction)	±3.4%	±2.2
Counting efficiency		
Volume efficiency	±1.0%	±0.7
End losses	±0.5%	±0.3
Monte Carlo interpolation	±0.3%	±0.2
Shifts of gain	−1.1%	+0.7
Resolution	+0.5%, −0.7%	−0.3, +0.5
Rise time limits	±1.0%	±0.7
Lead and exposure times	±0.8%	±0.5
Total (counting)	+1.8%, −2.1%	−1.2, +1.4
Nonsolar neutrino production of ^{71}Ge		
Fast neutrons		< −0.02
^{232}Th		< −0.04
^{226}Ra		< −0.7
Cosmic-ray muons		< −0.7
Total (nonsolar)		< −1.0
Background events that mimic ^{71}Ge		
Internal ^{222}Rn		< −0.2
External ^{222}Rn		0.0
Internal ^{69}Ge		< −0.6
Total (background events)		< −0.6
Energy weighting in analysis		±0.1
Total		−2.8, +2.6

in 2004 by sending the samples to Gran Sasso. In a cooperative effort [7], the GNO collaboration synthesized GeH_4 and measured the samples in their counting system.

The results for each individual extraction are tabulated in Appendix B and the combined result of each year of SAGE data since its beginning is shown in Figure 2.

The systematic uncertainties in the experiment have been considered in detail in [2, 3] and the most recent values are given in Table I. The only significant changes from our previous articles are due to the new proportional counters. Their high stability and efficiency have led to a considerable reduction of the errors associated with counting.

In radiochemical experiments the capture rate has been conventionally expressed in 'SNU units', defined as one neutrino capture per second in a target that contains 10^{36} atoms of the neutrino-absorbing isotope, in our case ^{71}Ga. For all SAGE data from January 1990 through December 2007 (168 runs and 310 separate counting sets) the global best fit capture rate is $65.4^{+3.1}_{-3.0}$ SNU, where the uncertainty is statistical only. If one considers the L-peak and K-peak data separately, the results are $67.2^{+4.8}_{-4.6}$ SNU and $64.0^{+4.1}_{-4.0}$ SNU, respectively. The agreement between the two peaks serves as a strong check on the robustness of the event selection criteria. Including the systematic uncertainty, our overall result is $65.4^{+3.1}_{-3.0}$ (stat)$^{+2.6}_{-2.8}$ (syst) SNU.

As further evidence that we are truly counting ^{71}Ge, we can allow the decay constant during counting to be a free variable in the maximum likelihood fit, along with the combined ^{71}Ge production rate and all the background rates. The best fit half-life to all selected events in both L and K peaks is then 11.5 ± 0.9 (stat) days, in agreement with the measured value [8] of 11.43 ± 0.03 days.

The waveform data from the Gallex experiment has recently been re-evaluated by Kaether using a new pulse-shape analysis method [9] and the result is $73.1^{+6.1+3.7}_{-6.0-4.1}$ SNU. The result of the GNO experiment was $62.9^{+5.5+2.5}_{-5.3-2.5}$ SNU [10]. If we combine the statistical and systematic uncertainties in quadrature, then the weighted combination of all the Ga experiments, SAGE, Gallex, and GNO, is

$$66.1 \pm 3.1 \text{ SNU.} \qquad \text{(Present Ga experiment result.)} \quad (1)$$

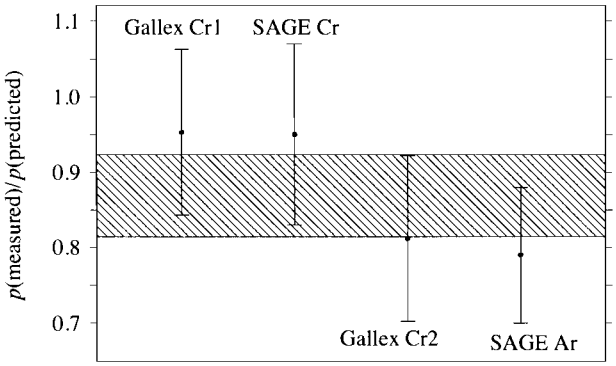

FIG. 3: Results of all neutrino source experiments with Ga. Gallex results are from the recent pulse shape analysis of Kaether [9]; SAGE results are from [11] and [4]. Hashed region is the weighted average of the four experiments.

IV. SOURCE EXPERIMENTS

The experimental procedures of the SAGE and Gallex experiments, including the chemical extraction, counting, and analysis techniques, have been checked by exposing the gallium target to reactor-produced neutrino sources whose activity was close to 1 MCi. SAGE has irradiated about 25% of their target with a ^{51}Cr source [11] and an ^{37}Ar source [4, 12, 13] and Gallex has twice used ^{51}Cr sources to irradiate their entire target [14]. The results, expressed as the ratio R of the measured ^{71}Ge production rate to that expected due to the source strength, are shown in Figure 3. The weighted average value of the ratio for the four experiments is $R = 0.88 \pm 0.05$, more than two standard deviations less than unity.

Since other auxiliary tests, especially the ^{71}As experiment of Gallex [15], have given great confidence in the knowledge of the various efficiencies in the Ga experiments, the combined result of these source tests should not be considered to be a measurement of the entire throughput of the Ga experiments. Rather, we believe that, although not statistically conclusive, the combination of these experiments suggests that the predicted rates may be overestimated. Although there are alternative explanations [1], a likely hypothesis is that the cross sections for neutrino capture to the lowest two excited states in ^{71}Ge, both of which can be reached using either ^{51}Cr or ^{37}Ar sources, have been overestimated [16]. If the contribution of these two excited states to the predicted rate is set to zero, then $R = 0.93 \pm 0.05$, reasonably consistent with unity.

Based on the information given in the definitive article of Bahcall [19] on the neutrino capture cross section of ^{71}Ga, we have approximately calculated the cross section if we assume zero strength for capture to the first two excited states of ^{71}Ge. These results are given in Appendix C and will be used in the next Section.

[1] See [17] for an explanation based on transitions to sterile neutrinos or [18] for a partial explanation based on quantum decoherence in neutrino oscillations.

TABLE II: Solar neutrino fluxes calculated by the standard solar model of Bahcall *et al.* [20, 21] for two different conservative choices of heavy element composition, labeled GS98 [22] (high metallicity) and AGS05 [23] (low metallicity). Units of flux are 10^{10} (*pp*), 10^9 (^{7}Be), 10^8 (*pep*, ^{13}N, ^{15}O), 10^6 (^{8}B, ^{17}F), and 10^3 (*hep*) cm^{-2}s^{-1}. The more recent values [21] are based on the new measurement of $S_{34}(0)$ by the LUNA experiment [24]. The uncertainty values are at 68% confidence.

Spectrum	Flux $\phi_i^{\odot}$			
comp. i	GS98 [20]	GS98 [21]	AGS05 [20]	AGS05 [21]
pp	$5.987(1^{+0.009}_{-0.009})$	$5.97(1^{+0.008}_{-0.008})$	$6.054(1^{+0.008}_{-0.008})$	$6.04(1^{+0.008}_{-0.008})$
pep	$1.419(1^{+0.015}_{-0.015})$	$1.41(1^{+0.013}_{-0.013})$	$1.451(1^{+0.013}_{-0.013})$	$1.46(1^{+0.013}_{-0.013})$
^{7}Be	$4.840(1^{+0.105}_{-0.105})$	$5.08(1^{+0.050}_{-0.050})$	$4.325(1^{+0.103}_{-0.103})$	$4.55(1^{+0.050}_{-0.050})$
^{13}N	$3.05(1^{+0.366}_{-0.268})$	$2.93(1^{+0.020}_{-0.150})$	$1.99(1^{+0.355}_{-0.262})$	$1.93(1^{+0.020}_{-0.150})$
^{15}O	$2.31(1^{+0.374}_{-0.272})$	$2.20(1^{+0.230}_{-0.160})$	$1.43(1^{+0.361}_{-0.265})$	$1.37(1^{+0.230}_{-0.160})$
^{17}F	$6.00(1^{+0.724}_{-0.420})$	$5.82(1^{+0.250}_{-0.250})$	$3.37(1^{+0.676}_{-0.404})$	$3.24(1^{+0.250}_{-0.250})$
^{8}B	$5.70(1^{+0.173}_{-0.147})$	$5.94(1^{+0.101}_{-0.101})$	$4.49(1^{+0.161}_{-0.141})$	$4.72(1^{+0.101}_{-0.101})$
hep	$7.970(1^{+0.155}_{-0.155})$	$7.90(1^{+0.154}_{-0.154})$	$8.281(1^{+0.153}_{-0.153})$	$8.22(1^{+0.154}_{-0.154})$

V. INTERPRETATION OF RESULTS

In contrast to all other present or past solar neutrino experiments, the radiochemical Ga experiment, because of its low threshold of 233 keV, is sensitive to all components of the solar spectrum, from the low-energy *pp* neutrinos to the high-energy neutrinos produced in the decay of ^{8}B. In Table II we give the flux of the various solar neutrino components at their production regions in the Sun as calculated by Bahcall and collaborators [20, 21]. In this Section we will estimate the neutrino capture rate from each flux component and compare their total to the measured rate.

The total capture rate R of solar neutrinos in a radiochemical experiment such as Ga is given by

$$R = \int_{E_{\rm threshold}}^{\infty} \sigma(E)\Phi^{\odot}(E)dE, \qquad (2)$$

where $\sigma(E)$ is the cross section of the neutrino-capture reaction and $\Phi^{\odot}(E)$ is the total flux of electron neutrinos at the Earth, which can be expressed as

$$\Phi^{\odot}(E) = \sum_i \phi_i^{\odot} S_i^{\odot}(E). \qquad (3)$$

In this expression the index i refers to the various nuclear reactions in the Sun that produce neutrinos (*pp*, ^{7}Be, *pep*, ^{13}N, ^{15}O, ^{17}F, ^{8}B, and *hep*), $\phi_i^{\odot}$ is the amplitude of flux component i at the Earth, and $S_i^{\odot}(E)$ is the spectrum of the ith neutrino component at the Earth, each of which is normalized such that $\int_0^{\infty} S_i^{\odot}(E)dE = 1$. The neutrino spectrum at the Earth is related to the spectrum produced in the Sun $S_i^{\odot}(E)$ by

$$S_i^{\odot}(E) = A_i S_i^{\odot}(E) P_i^{ee}(E), \qquad (4)$$

TABLE III: Factors needed to compute the solar neutrino capture rate in ^{71}Ga and ^{37}Cl solar neutrino experiments. The uncertainty values are at 68% confidence.

	Spect.		Percent uncertainty in $\langle P_i^{ee}\rangle$ due to			Total unc.	$\langle\sigma_i^{\odot}\rangle$	Percent uncertainty in $\langle\sigma_i^{\odot}\rangle$ due to				Total unc.
Exp.	comp.	$\langle P_i^{ee}\rangle$	Δm^2_{12}	θ_{12}	θ_{13}	in $\langle P_i^{ee}\rangle$ (%)	(10^{-46} cm^2)	σ	Δm^2_{12}	θ_{12}	θ_{13}	in $\langle\sigma_i^{\odot}\rangle$ (%)
^{71}Ga	*pp*	0.560	+0.0,-0.0	+3.0,-2.7	+0.0,-3.7	+3.0,-4.5	11.75	+2.4,-2.3	+0.0,-0.0	+0.0,-0.0	+0.0,-0.0	+2.4,-2.3
	pep	0.521	+0.2,-0.3	+2.4,-2.0	+0.0,-3.5	+2.5,-4.1	194.4	+17,-2.4	+0.0,-0.0	+0.0,-0.0	+0.0,-0.0	+17,-2.4
	^{7}Be	0.541	+0.1,-0.1	+2.8,-2.4	+0.0,-3.6	+2.8,-4.3	68.21	+7.0,-2.3	+0.0,-0.0	+0.0,-0.0	+0.0,-0.0	+7.0,-2.3
	^{13}N	0.544	+0.1,-0.1	+2.8,-2.4	+0.0,-3.6	+2.8,-4.4	56.84	+9.8,-2.3	+0.0,-0.0	+0.1,-0.1	+0.0,-0.0	+9.8,-2.3
	^{15}O	0.535	+0.2,-0.2	+2.7,-2.3	+0.0,-3.6	+2.7,-4.2	107.1	+13,-2.3	+0.0,-0.0	+0.1,-0.1	+0.0,-0.0	+13,-2.3
	^{17}F	0.535	+0.2,-0.2	+2.7,-2.3	+0.0,-3.6	+2.7,-4.2	107.7	+13,-2.3	+0.0,-0.0	+0.1,-0.1	+0.0,-0.0	+13,-2.3
	^{8}B	0.380	+0.5,-0.6	+3.5,-3.3	+0.0,-3.3	+3.6,-4.7	21770	+32,-14	+0.2,-0.2	+1.9,-2.2	+0.0,-0.1	+32,-15
	hep	0.355	+0.4,-0.4	+5.0,-4.8	+0.0,-3.4	+5.0,-5.9	66780	+33,-15	+0.2,-0.2	+1.2,-1.4	+0.0,-0.1	+33,-16
^{37}Cl	*pep*	0.521	+0.2,-0.3	+2.4,-2.0	+0.0,-3.5	+2.5,-4.1	16.00	+2.0,-2.0	+0.0,-0.0	+0.0,-0.0	+0.0,-0.0	+2.0,-2.0
	^{7}Be	0.541	+0.1,-0.1	+2.8,-2.4	+0.0,-3.6	+2.8,-4.3	2.397	+2.0,-2.0	+0.0,-0.0	+0.0,-0.0	+0.0,-0.0	+2.0,-2.0
	^{13}N	0.544	+0.1,-0.1	+2.8,-2.4	+0.0,-3.6	+2.8,-4.4	1.687	+2.0,-2.0	+0.1,-0.1	+0.2,-0.1	+0.0,-0.0	+2.0,-2.0
	^{15}O	0.535	+0.2,-0.2	+2.7,-2.3	+0.0,-3.6	+2.7,-4.2	6.668	+2.0,-2.0	+0.1,-0.1	+0.2,-0.2	+0.0,-0.0	+2.0,-2.0
	^{17}F	0.535	+0.2,-0.2	+2.7,-2.3	+0.0,-3.6	+2.7,-4.2	6.715	+2.0,-2.0	+0.1,-0.1	+0.2,-0.2	+0.0,-0.0	+2.0,-2.0
	^{8}B	0.380	+0.5,-0.6	+3.5,-3.3	+0.0,-3.3	+3.6,-4.7	10340	+3.7,-3.7	+0.2,-0.2	+2.2,-2.5	+0.0,-0.1	+4.3,-4.4
	hep	0.355	+0.4,-0.4	+5.0,-4.8	+0.0,-3.4	+5.0,-5.9	41440	+3.7,-3.7	+0.2,-0.2	+1.3,-1.5	+0.0,-0.1	+3.9,-4.0

where A_i is a constant of normalization and $P_i^{ee}(E)$ is the probability that an electron neutrino produced in the Sun by reaction i with energy E will reach the Earth without a change of flavor, commonly called the survival factor. The physical origin for the reduction of the electron component of the solar neutrino flux is the now well-established mechanism of MSW neutrino oscillations [25]. $P_i^{ee}(E)$ is different for each flux component as the neutrinos are produced at different locations in the Sun and thus pass through regions of different electron density during their travel to the Earth. $P_i^{ee}(E)$ can only be calculated if one knows where in the Sun the neutrinos are made and thus requires a solar model.

We integrate Eq. (4) and obtain $A_i = 1/\langle P_i^{ee}\rangle$ where

$$\langle P_i^{ee}\rangle = \int_0^{\infty} S_i^{\odot}(E) P_i^{ee}(E) dE \tag{5}$$

is the spectrum-weighted average value of P_i^{ee}. The physical interpretation of $\langle P_i^{ee}\rangle$ is as the ratio of the solar neutrino amplitudes at the surface of the Earth and at the production point in the Sun:

$$\langle P_i^{ee}\rangle = \frac{\phi_i^{\oplus}}{\phi_i^{\odot}}. \tag{6}$$

Combining these equations, and expressing R as the sum of its spectral components, $R = \sum_i R_i$, we have

$$R_i = \phi_i^{\odot}\langle\sigma_i^{\odot}\rangle \tag{7}$$

where

$$\langle\sigma_i^{\odot}\rangle = \int_{E_{\text{threshold}}}^{\infty} \sigma(E) S_i^{\odot}(E) P_i^{ee}(E) dE, \tag{8}$$

or, equivalently, if it the flux at the Earth that is assumed known,

$$R_i = \phi_i^{\oplus}\langle\sigma_i^{\oplus}\rangle, \tag{9}$$

where

$$\langle\sigma_i^{\oplus}\rangle = \frac{\langle\sigma_i^{\odot}\rangle}{\langle P_i^{ee}\rangle}. \tag{10}$$

In Table III we give values of $\langle P_i^{ee}\rangle$ and $\langle\sigma_i^{\oplus}\rangle$ for each neutrino component. These were calculated assuming three-neutrino mixing to active neutrinos with the parameters $\Delta m^2_{12} = (7.59 \pm 0.21) \times 10^{-5}$ eV^2, $\theta_{12} = 34.5 \pm 1.4$ degrees, and $\theta_{13} = 0.0^{+7.9}_{-0.0}$ degrees [26, 27]. The approximate formulae given in [28] were used for the survival probability $P_i^{ee}(E)$. Since radiochemical experiments average over a long exposure interval, regeneration in the Earth was neglected. The cross sections $\sigma(E)$ were taken from Appendix C for Ga and Ref. [29] for Cl. The neutrino spectra $\phi_i^{\odot}(E)$ are from [19] (*pp*, ^{13}N, ^{15}O, ^{17}F), [29] (^{8}B), and [30] (*hep*).

Now that all the terms have been calculated, we can use the fluxes in Table IV, combined with Eq's (7) and (10), to predict the capture rate in Ga from each of the solar neutrino components. The individual rates and the total rate are given in Table IV for two recent solar models from Table II. For both models there is good agreement between the calculated total rate and the observed capture rate of 66.1 ± 3.1 SNU. The major contributions to the uncertainty in the predicted total rate are from the solar model fluxes and the neutrino capture cross section, with smaller contributions from θ_{12} and θ_{13}.

In this analysis we have used the cross sections in Appendix C, in which the contribution of the two lowest-lying excited states in ^{71}Ge has been set to zero. If instead we use the original Bahcall cross sections, then the total rate increases by 1.2 SNU with the GS98 composition and by 1.1 SNU with the AGS05 composition. Whatever cross sections are assumed is thus not a significant factor in the interpretration of the total rate in the Ga experiment. The cross sections are, however, of vital importance in understanding the origin of the unexpectedly low result in the source experiments.

VI. THE *pp* NEUTRINO FLUX FROM THE SUN

In this section we will use the Ga measurement given in Eq. (1) and the results of other solar neutrino experiments to determine the *pp* flux from the Sun. Strictly speaking, this cannot really be done with the data now available as the capture rate in the Ga experiment has contributions from all the

TABLE IV: Capture rates R_i for Ga experiments calculated with fluxes from Ref. [21].

	With GS98 composition							With AGS05 composition						
Spect.	Cap. rate	Percent uncertainty in rate due to					Total unc.	Cap. rate	Percent uncertainty in rate due to					Total unc.
comp.	(SNU)	ϕ	σ	Δm^2_{12}	θ_{12}	θ_{13}	in rate (%)	(SNU)	ϕ	σ	Δm^2_{12}	θ_{12}	θ_{13}	in rate (%)
pp	39.27	+0.8,-0.8	+2.4,-2.3	+0.0,-0.0	+3.0,-2.7	+0.0,-3.7	+3.9,-5.1	39.73	+0.8,-0.8	+2.4,-2.3	+0.0,-0.0	+3.0,-2.7	+0.0,-3.7	+3.9,-5.1
pep	1.43	+1.3,-1.3	+17.0,-2.4	+0.2,-0.3	+2.4,-2.0	+0.0,-3.5	+17.2,-4.9	1.48	+1.3,-1.3	+17.0,-2.4	+0.2,-0.3	+2.4,-2.0	+0.0,-3.5	+17.2,-4.9
^{7}Be	18.75	+5.0,-5.0	+7.0,-2.3	+0.1,-0.1	+2.8,-2.4	+0.0,-3.6	+9.1,-7.0	16.79	+5.0,-5.0	+7.0,-2.3	+0.1,-0.1	+2.8,-2.4	+0.0,-3.6	+9.1,-7.0
^{13}N	0.91	+20.0,-15.0	+9.8,-2.3	+0.1,-0.1	+2.8,-2.4	+0.0,-3.6	+22.4,-15.8	0.60	+20.0,-15.0	+9.8,-2.3	+0.1,-0.1	+2.8,-2.4	+0.0,-3.6	+22.4,-15.8
^{15}O	1.26	+23.0,-16.0	+12.9,-2.3	+0.2,-0.2	+2.6,-2.2	+0.0,-3.5	+26.5,-16.7	0.78	+23.0,-16.0	+12.9,-2.3	+0.2,-0.2	+2.6,-2.2	+0.0,-3.5	+26.5,-16.7
^{17}F	0.03	+25.0,-25.0	+12.9,-2.3	+0.2,-0.2	+2.6,-2.2	+0.0,-3.5	+28.3,-25.4	0.02	+25.0,-25.0	+12.9,-2.3	+0.2,-0.2	+2.6,-2.2	+0.0,-3.5	+28.3,-25.4
^{8}B	4.91	+10.1,-10.1	+31.8,-14.4	+0.4,-0.4	+5.5,-5.4	+0.0,-3.4	+33.8,-18.7	3.90	+10.1,-10.1	+31.8,-14.4	+0.4,-0.4	+5.5,-5.4	+0.0,-3.4	+33.8,-18.7
hep	0.02	+15.4,-15.4	+32.7,-15.4	+0.2,-0.2	+6.3,-6.1	+0.0,-3.5	+36.7,-22.9	0.02	+15.4,-15.4	+32.7,-15.4	+0.2,-0.2	+6.3,-6.1	+0.0,-3.5	+36.7,-22.9
Total	66.58	+1.7,-1.7	+3.4,-1.8	+0.1,-0.1	+2.0,-1.8	+0.0,-2.4	+4.3,-3.9	63.32	+1.6,-1.6	+3.1,-1.8	+0.0,-0.0	+2.0,-1.8	+0.0,-2.5	+4.1,-3.9

components of the solar neutrino spectrum, and thus it is only possible to separate out the portion from *pp* when other experiments have measured the electron-neutrino part of all the other flux components. Nevertheless, the *pp* flux can be obtained from the present experiments if we make some reasonable approximations.

The rate in Eq. (1) is the sum of the rates from all the components of the solar neutrino flux, which we denote by

$$[pp+^7\text{Be}+\text{CNO}+pep+^8\text{B}|\text{Ga}] = 66.1(1 \pm 0.047)\ \text{SNU}. \quad (11)$$

We ignore the tiny *hep* contribution and combine the ^{13}N, ^{15}O, and ^{17}F components into a single value, called here 'CNO'.

In an experiment of great technical difficulty, the ^{7}Be flux has been directly measured by Borexino and they report the result as $\phi^{\odot}_{^7\text{Be}} = 5.18(1 \pm 0.098) \times 10^9$ neutrinos/(cm^2 s) [31]. Using Eq. (7) and (10), we multiply this flux by the electron neutrino survival factor for ^{7}Be and by the cross section of ^{7}Be on Ga (the values of these factors and their uncertainties are given in Table III) and obtain the rate of ^{7}Be in Ga of

$$[^7\text{Be}|\text{Ga}] = 19.1(1^{+0.12}_{-0.11})\ \text{SNU}. \quad (12)$$

The ^{8}B flux at the Earth has been directly measured by SNO to be $\phi^{\dagger}_{^8\text{B}} = (1.67 \pm 0.05) \times 10^6$ electron neutrinos/(cm^2 s) [32]. In a similar way to ^{7}Be, we multiply this flux by the spectrum-integrated cross section for ^{8}B neutrinos on Ga and obtain the ^{8}B contribution to the Ga experiment of

$$[^8\text{B}|\text{Ga}] = 3.6(1^{+0.32}_{-0.16})\ \text{SNU}. \quad (13)$$

Subtracting these measured rates of ^{7}Be and ^{8}B from the total Ga rate in Eq. (11) gives

$$[pp+\text{CNO}+pep|\text{Ga}] = 43.3(1^{+0.087}_{-0.094})\ \text{SNU}. \quad (14)$$

We can obtain an approximate value for the contribution of CNO and *pep* to the Ga experiment from the measured capture rate in the Cl experiment [^{7}Be+CNO+*pep*+^{8}B|Cl] = 2.56(1 ± 0.088) SNU [1]. As in the case of Ga, we use the ^{7}Be flux measured by Borexino, the ^{8}B flux measured by SNO, and the cross sections in Table III to determine [^{7}Be|Cl] = $0.67(1^{+0.104}_{-0.109})$ SNU and [^{8}B|Cl] = $1.73(1^{+0.067}_{-0.069})$ SNU. We subtract these values from the total Cl rate and are left with [CNO+*pep*|Cl] = $0.16(1^{+1.65}_{-1.00})$ SNU.

If we attribute this entire rate to the neutrinos from *pep* then, using the cross sections for *pep* on Cl and Ga, we calculate a rate of $[pep|\text{Ga}]_{\text{test}} = 1.96(1^{+1.66}_{-1.00})$ SNU. On the other hand, if we attribute this entire rate to CNO, we obtain in the same manner a rate of $[\text{CNO}|\text{Ga}]_{\text{test}} = 2.59(1^{+1.65}_{-1.00})$ SNU. The upper extreme of these two test rates is 2.59 × 2.65 = 6.86 SNU. As a reasonable estimate we can thus set the sum of CNO and *pep* rates at half this upper limit with an uncertainty of 100%:

$$[\text{CNO}+pep|\text{Ga}] = 3.43(1^{+1.00}_{-1.00})\ \text{SNU}. \quad (15)$$

We subtract this estimate for the CNO plus *pep* rate from the rate in Eq. (14) and obtain the result for the measured *pp* rate in the Ga experiment

$$[pp|\text{Ga}] = 39.9(1 \pm 0.13)\ \text{SNU}. \quad (16)$$

Dividing this capture rate by the cross section for capture of *pp* neutrinos gives the measured electron neutrino *pp* flux at Earth of

$$\phi^{\dagger}_{pp} = 3.40(1^{+0.13}_{-0.14}) \times 10^{10}/(\text{cm}^2\ \text{s}). \quad (17)$$

If we use Eq. (6) and the value of $\langle P^{ee}_i \rangle = 0.560(1^{+0.030}_{-0.045})$ from Table III then the *pp* flux produced in the Sun is

$$\phi^{\odot}_{pp} = 6.1(1 \pm 0.14) \times 10^{10}/(\text{cm}^2\ \text{s}). \quad (18)$$

Our present result for the *pp* flux is in good agreement with the previous estimates that we have made during the last six years [3, 33, 34], with the major change being a gradual reduction of the uncertainty. In the future, as Borexino continues to collect data, and as direct measurements are made of the CNO and *pep* fluxes, the uncertainty in this flux should be further reduced, and eventually may be dominated by the error in the Ga rate itself. By that time, however, there will hopefully be direct experiments that measure the *pp* flux in real time.

For comparison, we see from Table II that the predicted *pp* flux from the two recent solar models with different composition is $\phi^{\odot}_{pp} = 5.97 \pm 0.05$ and 6.04 ± 0.05, both in units of 10^{10} ν_e/(cm^2 s). There is good numerical agreement between these flux values and the result in Eq. (18), but, as made clear by Bahcall and Peña-Garay [35], there is a large difference in interpretation: the result in Eq. (18) was derived from contemporary solar neutrino experiments and is the *pp* neutrino flux

at the present time. In contrast, energy generation in the solar model is highly constrained by the measured solar luminosity and thus, when the luminosity constraint is imposed, as is the case for the models given in Table II, the calculated *pp* flux is what the Sun was making some 40 000 years ago.

VII. CONSIDERATION OF TIME VARIATION

In a plot of the SAGE results as a function of time there is a slight visual hint of a long-term decrease, as illustrated in Figure 2. The average rate prior to 1996 is somewhat higher than after 1996. A plot of the Gallex-GNO data shows a similar behavior [10]. When examined quantitatively, however, the evidence for a long-term decrease in the capture rate is unconvincing. A χ^2 test applied to these yearly SAGE data points assuming the rate is constant at 65.4 SNU gives χ^2/dof = 12.0/17, which has a probability of 80%. The fit to a constant rate is thus quite good.

In previous articles we have demonstrated the agreement between the assumption of a constant production rate and the SAGE measurements by use of the cumulative distribution of the production rate $C(p)$, defined as the fraction of data sets whose production rate is less than p. Figure 4 shows this distribution for the data and the expected distribution derived from 100 simulations of all 168 runs, where it is assumed in the simulations that the production rate is constant and has a value of 65.4 SNU. For each run the rates from the separate L and K peaks are used in this Figure, not the rate from the $L+K$ combination. To ensure that the simulations parallel the real data as closely as possible, all parameters of the simulation, such as background rates, efficiencies, exposure times, and counting times, were chosen to be the same as for the real data. Only the number of counts in each run and the times when these counts occurred were allowed to vary.

The data spectrum and the simulated spectrum are very similar to each other, indicating that the distribution of production rates is what one would expect if the rate is constant. A quantitative comparison can be made by calculating the Nw^2 test statistic [36]. (This test is similar to a Kolmogorov-Smirnov test, but has the advantage that the data are not binned.) The value of Nw^2 for the data distribution is 0.520, very close to the mean value of Nw^2 from the 100 simulations of 0.513. The fraction of simulations whose Nw^2 was larger than for the data was 43%, thus showing that the assumption of a constant production rate is in good agreement with our measurements.

A standard method to look for periodic signals in unevenly sampled data, such as we have in SAGE, was devised by Lomb and Scargle. Application of this method, using the implementation of Press *et al.* [37], to all runs from the SAGE experiment yields the power spectrum shown in Figure 5. The frequency range considered is from nearly zero up to slightly less than twice the Nyquist frequency. The maximum Lomb power is 6.10 and it occurs at a frequency of 8.47 cycles/year.

A simple way to assess the significance of a peak in such a spectrum is to make a histogram of the number of frequencies as a function of power. In the absence of any time variation this distribution is an exponential; if there were any peak

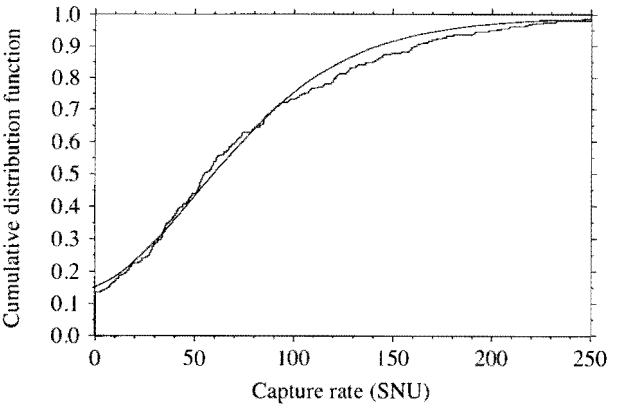

FIG. 4: Measured capture rate for all 310 SAGE data sets (jagged curve) and the expected distribution derived by 100 Monte Carlo simulations of each set (smooth curve).

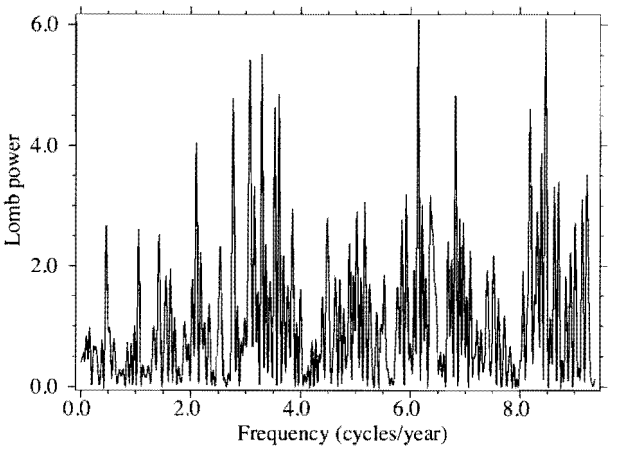

FIG. 5: Lomb power spectrum from all 168 SAGE data runs. The mean time of exposure was used as the time of measurement.

present with significant power it would appear at the upper end of the distribution and be clearly separated from the exponential trend. This distribution for the spectrum of Figure 5 is shown in Figure 6. There is no evidence for exceptional power in the data spectrum at any frequency.

An alternative way to evaluate the significance of a frequency with high power is with a shuffle test. In this test the SNU results are randomly re-assigned to the different runs, the power spectrum is recalculated, and the maximum power is found. The maximum power in the spectra from 1000 such shuffles is plotted in Figure 7. The observed maximum power for the SAGE data of 6.10 occurs very near the center of this distribution. 44% of the shuffles have a greater power than for the data and 56% a lesser power, thus showing that the observed power distribution is consistent with the assumption of a constant rate.

The same result is obtained if power spectra are produced over a wider frequency range. For ranges up to 19 per year and 38 per year the maximum power remains 6.10 at 8.47 cy-

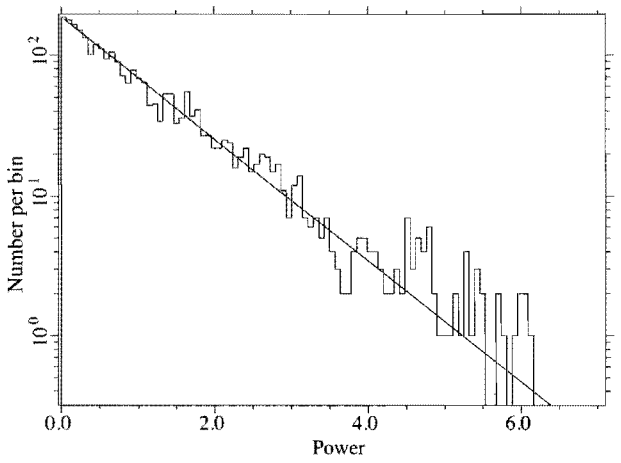

FIG. 6: Histogram of powers in spectrum of Fig. 5. The bin size is 0.07 power units. The solid line is the expected distribution if there is no time variation, i.e., the number of frequencies × exp(−power), integrated over the limits of each bin.

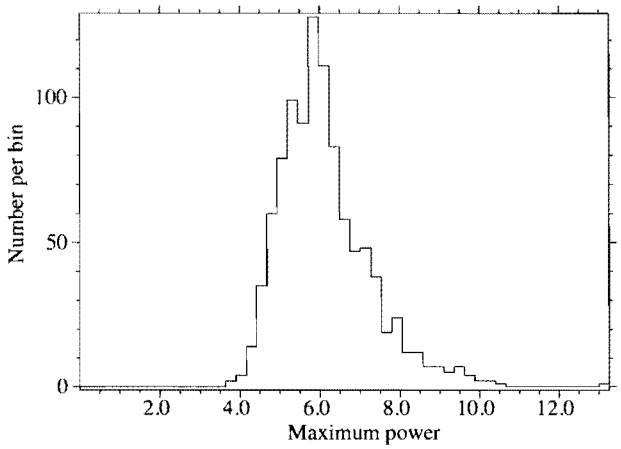

FIG. 7: Histogram of maximum power found in Lomb power spectrum analysis of 1000 random shuffles of the 168 SAGE runs. The bin size is 0.13 power units.

cles/year and is not statistically significant.

VIII. SUMMARY AND DISCUSSION

In 18 years of operation the SAGE experiment has carried out 168 measurements of the solar neutrino capture rate. Analysis of the times of occurrence of all events in windows centered on the L and K peaks and with 2 FWHM width ascribes 853.9 of these events to the decay of ^{71}Ge. To compare these values with other radiochemical solar neutrino experiments, the Cl experiment collected solar data for a longer time (108 runs with rise-time counting during 24 years), but the number of detected events within an energy window of 2 FWHM that were ascribed to ^{37}Ar was 875 [1], quite comparable to what we now have in SAGE. So far as we are aware, neither Gallex nor GNO have reported their total number of detected ^{71}Ge events, but since the mass of their Ga target was less (30 tonnes), and their number of runs was less (123 during 12 years), this number must be considerably lower than we now have in SAGE.

The measured best-fit capture rate in the SAGE experiment is $65.4^{+3.1}_{-3.0}$ (stat) $^{+2.6}_{-2.8}$ (syst) SNU. Combining this with the results of Gallex and GNO gives the rate as 66.1 ± 3.1 SNU, where statistical and systematic uncertainties have been combined in quadrature. The solar-model prediction for the Ga experiment is 66.6 SNU for a model with high metallicity and 63.3 SNU for a model with low metallicity, where the error of both estimates is ~5%. There is thus excellent agreement between theory and experiment for the Ga experiment. Further, both the experimental measurement and the theoretical prediction are known to about the same accuracy.

By use of the results of other solar neutrino experiments and neutrino oscillation theory we have derived the contemporary value of the pp flux from the Sun to be $(3.40^{+0.44}_{-0.46}) \times 10^{10}$/(cm^2 s) at the Earth and (6.1 ± 0.8) × 10^{10}/(cm^2 s) at the Sun. The latter is in good agreement with standard solar model predictions of 5.97 ± 0.05 (high metallicity) and 6.04 ± 0.05 (low metallicity), both in units of 10^{10} ν_e/(cm^2 s). Gallium experiments have thus proven that the overwhelming fraction of solar neutrinos that reach the Earth are the low-energy neutrinos from the pp reaction.

We have assumed in these calculations that the cross section for capture to the two lowest-lying excited states in ^{71}Ge is zero, as is implied by the four neutrino source experiments with gallium. This assumption is in contradiction to the standard interpretation of the two experiments that have attempted to measure the Gamow-Teller strength of these low-lying excited states in ^{71}Ge. These experiments were made by (p,n) scattering [19, 38] and (^{3}He,t) scattering [39–41]. If all the events observed in these experiments at low excitation energy are attributed to Gamow-Teller strength the results of these experiments are in reasonably good agreement. It is, however, not evident that these experiments solely measure Gamow-Teller strength – as emphasized by Haxton [16], for very weak transitions, such as is the case in these experiments, there may be an appreciable (perhaps dominant) contribution to the cross section from the spin-tensor interaction. New experimental data is needed to settle this question and to definitively determine the magnitude of the matrix elements for neutrino capture to these two low-lying excited states. We strongly encourage any new experiments that might shed light on this question. As part of our future experimental program we intend to pursue a new measurement that will use a very intense neutrino source in an optimized detector geometry.

The SAGE experiment continues to collect data on the solar neutrino capture rate with a gallium target. Up to now it is only the Ga experiment that has measured the low-energy pp solar neutrinos. As we continue to monitor the solar neutrino flux we will increase our statistical accuracy and further reduce our systematic uncertainties.

Acknowledgments

SAGE is grateful to M. Baldo-Ceolin, W. Haxton, V. A. Kuzmin, V. A. Matveev, S. P. Mikheev, R. G. H. Robertson, V. A. Rubakov, A. Yu. Smirnov, A. Suzuki, A. N. Tavkhelidze, and our colleagues from the GALLEX and GNO collaborations for their continued interest and for fruitful and stimulating discussions. We especially thank W. Hampel for vital comments on many aspects of our investigations.

SAGE acknowledges the support of the Russian Academy of Sciences, the Ministry of Education and Science of the Russian Federation, the Division of Nuclear Physics of the U. S. Department of Energy, and the U. S. National Science Foundation.

This work was partially funded by the Russian Foundation for Basic Research under grants No. 99-02-16110, No. 02-02-16776 and No. 05-02-17199, by the Program of President of the Russian Federation under grants No. 00-1596632, No. NS-1782.2003, and No. NS-5573.2006.2, the Program of Fundamental Research "Neutrino Physics" of the Presidium of the Russian Academy of Sciences, and by the International Science and Technology Center under grant No. 1431.

APPENDIX A: CALCULATION OF EXTRACTION EFFICIENCY FROM ISOTOPIC ANALYSIS

It is assumed the extracted Ge consists of a combination of

- Ge from the carrier added for the current extraction,
- residual Ge that remained from the carrier added for the two preceding extractions, and
- additional Ge with natural isotopic composition, such as may be dissolved from the surfaces of the extraction system or the vessels that contain the Ga.

According to this model the predicted mass of isotope i obtained in extraction n, called $M_n^p(i)$, is thus

$$M_n^p(i) = \varepsilon_n\{C_n(i) + (1-\varepsilon_{n-1})[C_{n-1}(i) + (1-\varepsilon_{n-2})C_{n-2}(i)]\} + E_n I(i), \quad \text{(A1)}$$

where ε_m is the efficiency of Ge removal in extraction m, $C_m(i)$ is the mass of isotope i of carrier added to extraction m (where m can take on the values n, $n-1$, or $n-2$), and E_n is the mass of additional Ge with natural isotopic composition $I(i)$ that is removed in extraction n. It is assumed that $I(i)$, $C_n(i)$, $C_{n-1}(i)$, and $C_{n-2}(i)$ are known and the variables ε_n, ε_{n-1}, ε_{n-2}, and E_n are to be determined. For N extractions there are thus $2N$ variables (the extraction efficiency and mass of extra natural Ge for each extraction) and $5N$ equations that relate these variables, one for each of the naturally-occurring Ge isotopes, ^{70}Ge, ^{72}Ge, ^{73}Ge, ^{74}Ge, and ^{76}Ge. Since there are more relationships than unknowns, the problem is solved by finding the set of variables that minimizes the function

$$\chi^2 = \sum_{n=1}^{N}\sum_{i=1}^{5}\left(\frac{M_n^p(i) - M_n^e(i)}{\sigma_n(i)}\right)^2, \quad \text{(A2)}$$

where $M_n^e(i)$ is the measured mass of isotope i in extraction n and $\sigma_n(i)$ is the total uncertainty in the knowledge of the predicted and measured masses in extraction n.

APPENDIX B: RESULTS FOR EACH SAGE EXTRACTION

The capture rate for each SAGE extraction is given in Table V. The statistic Nw^2 in this Table measures the goodness of fit between the observed sequence of events in time and the time distribution predicted by the model used in analysis, viz., that the events are produced by the sum of two processes: the decay of a fixed initial number of ^{71}Ge atoms and background events at a constant rate. The probability to obtain the observed time distribution is given in the last column. It is derived from Nw^2 by 1000 simulations for each extraction using the method in [36] and has an uncertainty of ~1.5%.

TABLE V: Results of analysis of SAGE extractions.

Exposure date	Mean exposure date	Exposure time (days)	Ga mass (tons)	Number of candidate events	Number fit to ^{71}Ge	Best fit (SNU)	68% conf. range (SNU)	Nw^2	Probability (%)
Jan. 90	1990.040	42.0	28.67	8	0.6	0	0– 65	0.532	2
Feb. 90	1990.139	30.0	28.59	2	2.0	74	19–160	0.167	25
Mar. 90	1990.218	26.0	28.51	10	1.6	40	0–211	0.040	83
Apr. 90	1990.285	19.0	28.40	11	0.5	0	0–157	0.119	35
July 90	1990.540	21.0	21.01	13	0.3	0	0–252	0.080	50
June 91	1991.463	53.0	27.43	10	0.7	0	0–120	0.188	20
July 91	1991.539	23.0	27.37	1	1.0	34	0–116	0.163	33
Aug. 91	1991.622	26.3	49.33	16	9.9	395	247–584	0.036	85
Sep. 91	1991.707	27.0	56.55	11	3.1	42	9–123	0.023	97
Nov. 91	1991.872	26.0	56.32	31	4.2	61	9–162	0.173	12

Dec. 91	1991.948	26.8	56.24	10	10.0	159	100–219	0.061	79
Feb. 92-1	1992.138	24.5	43.03	14	0.8	0	0– 43	0.108	44
Feb. 92-2	1992.138	24.5	13.04	1	1.0	80	0–193	0.084	87
Mar. 92	1992.214	20.9	55.96	24	12.6	285	203–414	0.077	36
Apr. 92	1992.284	23.5	55.85	15	2.3	34	13–112	0.143	20
May 92	1992.383	27.5	55.72	5	0.7	0	0– 86	0.142	33
Sep. 92	1992.700	116.8	55.60	11	6.5	84	52–125	0.120	24
Oct. 92	1992.790	27.2	55.48	18	3.3	31	7– 63	0.093	37
Nov. 92	1992.871	26.7	55.38	28	6.9	90	45–145	0.143	13
Dec. 92	1992.945	24.3	55.26	27	17.6	174	121–229	0.063	57
Jan. 93	1993.039	32.3	55.14	17	9.9	122	74–176	0.093	33
Feb. 93	1993.115	23.0	55.03	3	0.8	18	0– 56	0.090	47
Apr. 93	1993.281	26.6	48.22	7	2.3	56	15–106	0.038	90
May 93	1993.364	30.9	48.17	8	0.6	28	0–122	0.115	41
June 93	1993.454	30.4	54.66	18	5.1	63	22–116	0.426	0
July 93	1993.537	27.9	40.44	28	6.7	198	100–312	0.041	84
Aug. 93-1	1993.631	34.0	40.36	4	2.7	73	28–125	0.051	81
Aug. 93-2	1993.628	63.8	14.09	1	1.0	120	0–230	0.093	75
Oct. 93-1	1993.749	13.0	14.06	0	0.0	0	0–158	NA	NA
Oct. 93-2	1993.800	34.7	14.10	4	3.1	144	71–246	0.052	86
Oct. 93-3	1993.812	24.6	14.02	6	2.9	132	64–231	0.049	82
July 94	1994.551	31.3	50.60	20	4.5	63	29–108	0.018	100
Aug. 94	1994.634	31.0	50.55	25	3.6	42	14– 79	0.031	95
Sep. 94-1	1994.722	33.2	37.21	30	5.9	101	42–174	0.100	36
Oct. 94	1994.799	28.8	50.45	44	0.0	0	0–128	0.269	12
Nov. 94	1994.886	31.0	50.40	23	8.0	115	68–172	0.015	100
Dec. 94	1994.951	21.0	13.14	9	0.0	0	0–236	0.184	20
Mar. 95	1995.209	42.5	24.03	23	3.6	145	48–264	0.042	84
July 95	1995.538	19.9	50.06	33	7.3	106	53–168	0.108	28
Aug. 95	1995.658	46.7	50.00	21	7.5	105	62–158	0.081	43
Sep. 95	1995.742	28.8	49.95	33	1.3	29	0–126	0.058	75
Oct. 95	1995.807	18.7	49.83	25	5.8	148	62–254	0.037	89
Nov. 95	1995.875	25.8	49.76	31	10.6	131	83–188	0.028	94
Dec. 95-2	1995.962	32.7	41.47	39	1.6	39	0–117	0.093	50
Jan. 96	1996.045	29.7	49.64	34	0.0	0	0– 42	0.095	53
May 96	1996.347	49.9	49.47	16	4.7	70	25–127	0.028	98
Aug. 96	1996.615	45.0	49.26	21	4.9	77	31–134	0.075	49
Oct. 96	1996.749	45.8	49.15	21	5.9	82	46–127	0.053	70
Nov. 96	1996.882	48.7	49.09	28	1.6	22	0– 64	0.097	45
Jan. 97	1997.019	49.8	49.04	24	2.8	37	6– 79	0.197	13
Mar. 97	1997.151	44.9	48.93	23	1.6	19	0– 55	0.457	1
Apr. 97	1997.277	42.9	48.83	22	3.2	41	12– 79	0.049	79
June 97	1997.403	45.6	48.78	26	10.3	140	91–199	0.073	43
July 97	1997.537	45.9	48.67	22	1.6	22	0– 56	0.445	1
Sep. 97	1997.671	46.4	48.56	15	3.9	62	25–110	0.036	91
Oct. 97	1997.803	45.0	48.45	25	4.6	63	28–108	0.127	23
Dec. 97	1997.940	47.0	48.34	22	4.7	78	34–135	0.054	66
Apr. 98	1998.225	44.9	48.05	38	5.8	82	35–140	0.048	77
May 98	1998.347	30.0	51.17	21	4.4	57	24– 98	0.036	90
July 98	1998.477	45.6	51.06	21	5.7	72	36–118	0.076	46
Aug. 98	1998.611	45.7	50.93	31	4.1	52	20– 95	0.047	82
Oct. 98	1998.745	45.8	50.81	38	4.7	56	18–103	0.027	96
Nov. 98	1998.883	45.8	50.68	30	5.2	59	20–107	0.078	51
Jan. 99	1999.014	44.7	50.54	21	2.3	29	0– 72	0.084	51
Feb. 99	1999.130	38.7	50.43	15	2.3	34	4– 76	0.096	42
Apr. 99	1999.279	51.7	50.29	9	1.5	33	5– 74	0.054	76

June 99	1999.417	46.7	50.17	14	14.0	185	140–239	0.031	98
July 99	1999.551	45.7	50.06	17	6.0	111	54–182	0.100	32
Sep. 99	1999.685	45.7	49.91	20	3.3	42	5– 93	0.250	5
Oct. 99	1999.801	38.7	49.78	15	9.6	134	81–196	0.082	49
Jan. 00	2000.035	28.8	49.59	23	7.3	84	46–129	0.101	30
Feb. 00	2000.127	30.7	49.48	20	7.9	92	55–138	0.044	80
Mar. 00	2000.207	28.8	49.42	18	9.3	106	70–150	0.051	72
May 00	2000.359	30.7	49.24	12	1.6	16	0– 43	0.048	85
June 00	2000.451	33.7	49.18	16	0.8	13	0– 59	0.324	6
July 00	2000.540	32.0	49.12	27	6.2	66	33–107	0.083	42
Aug. 00	2000.626	31.3	49.06	14	5.2	74	41–116	0.088	37
Sep. 00	2000.704	27.7	49.00	30	9.0	107	62–160	0.091	36
Oct. 00	2000.796	30.7	48.90	14	0.3	4	0– 31	0.090	56
Nov. 00	2000.876	28.7	48.84	22	1.0	11	0– 41	0.166	24
Dec. 00	2000.958	30.7	48.78	25	7.4	78	43–119	0.066	64
Feb. 01	2001.122	29.8	41.11	20	6.5	80	47–123	0.100	29
Mar. 01	2001.214	33.4	48.53	17	2.3	26	0– 66	0.077	55
Apr. 01	2001.290	22.7	48.43	16	6.7	70	41–107	0.087	40
May 01	2001.373	31.7	48.37	20	12.0	118	85–158	0.090	35
June 01	2001.469	31.7	48.27	19	7.2	66	38– 99	0.047	77
July 01	2001.547	23.7	48.17	7	3.0	36	17– 65	0.026	98
Aug. 01	2001.624	28.7	48.11	17	7.0	117	66–180	0.082	41
Sep. 01	2001.701	27.7	48.06	10	2.5	24	4– 52	0.126	22
Oct. 01	2001.793	30.7	47.96	12	7.0	63	39– 94	0.120	23
Nov. 01	2001.887	34.8	47.91	19	4.7	39	17– 67	0.104	29
Dec. 01	2001.955	22.8	47.86	20	4.4	47	22– 80	0.056	72
Jan. 02	2002.043	29.7	47.75	31	23.2	201	153–254	0.162	18
Feb. 02	2002.120	27.7	41.01	12	7.3	78	48–114	0.121	24
Mar. 02	2002.199	28.8	47.62	15	6.2	53	28– 84	0.090	35
Apr. 02	2002.291	30.7	47.51	13	2.7	25	10– 46	0.127	28
May 02	2002.354	20.7	47.45	23	6.0	63	31–104	0.024	99
June 02	2002.448	36.8	47.40	30	7.7	67	39–101	0.089	38
July 02	2002.541	29.7	47.30	16	2.0	20	0– 50	0.070	60
Aug. 02	2002.619	27.7	47.24	18	12.7	126	91–168	0.027	97
Sep. 02	2002.698	28.7	47.18	14	7.8	74	48–107	0.035	91
Oct. 02	2002.790	30.8	47.07	16	4.7	42	19– 70	0.030	96
Nov. 02	2002.868	27.8	42.54	48	6.0	61	24–106	0.073	59
Dec. 02	2002.947	28.8	49.58	25	4.7	46	19– 81	0.044	84
Jan. 03	2003.040	30.8	49.51	15	6.9	59	37– 86	0.106	27
Feb. 03	2003.117	27.7	49.44	20	5.9	53	27– 86	0.071	50
Mar. 03	2003.199	29.8	49.38	21	8.0	70	44–103	0.093	31
Apr. 03	2003.284	27.7	49.27	22	4.7	54	27– 89	0.122	23
May 03	2003.366	29.7	49.21	13	7.1	66	37–102	0.084	40
June 03	2003.448	29.7	49.16	17	10.4	114	77–159	0.077	46
July 03	2003.538	29.8	49.05	21	10.1	106	67–154	0.068	48
Aug. 03	2003.628	32.7	48.94	19	2.9	32	4– 67	0.029	96
Sep. 03	2003.713	30.7	48.94	11	0.0	0	0– 15	0.065	74
Oct. 03	2003.793	24.5	48.83	20	10.0	104	69–147	0.057	64
Nov. 03	2003.866	26.7	35.64	18	3.6	47	20– 85	0.135	23
Nov. 03-1	2003.875	26.2	13.11	10	2.4	84	11–187	0.066	71
Dec. 03	2003.945	27.5	35.61	11	5.9	78	43–123	0.113	27
Dec. 03-1	2003.960	26.9	13.07	10	2.1	77	13–170	0.023	99
Jan. 04	2004.037	30.8	35.54	19	0.0	0	0– 24	0.045	89
Jan. 04-1	2004.053	17.3	13.00	7	2.4	132	44–278	0.077	70
Feb. 04	2004.131	34.8	35.43	14	5.1	62	30–102	0.098	41
Feb. 04-1	2004.145	18.3	13.01	10	3.5	151	43–287	0.091	46
Mar. 04	2004.212	28.8	35.37	22	4.6	59	28–101	0.097	39
Mar. 04-1	2004.226	30.8	12.99	8	0.0	0	0–163	0.200	28
Apr. 04	2004.289	23.6	48.29	19	4.3	67	30–116	0.076	41

May 04	2004.354	23.4	22.03	9	3.6	78	25–148	0.076	46
June 04	2004.455	38.5	22.00	10	4.1	98	34–182	0.091	32
July 04	2004.544	24.9	21.95	14	2.0	43	0–118	0.051	74
Aug. 04	2004.623	29.3	21.93	12	5.2	139	80–218	0.048	82
Sep. 04	2004.712	32.9	42.42	14	0.1	0	0– 25	0.103	42
Oct. 04	2004.800	28.8	47.67	11	1.9	22	1– 50	0.074	56
Nov. 04-1	2004.881	29.7	47.62	17	7.3	73	43–111	0.037	87
Dec. 04	2004.954	25.6	47.57	45	25.3	305	238–381	0.025	96
Jan. 05	2005.047	31.7	47.47	14	1.4	12	0– 30	0.083	52
Feb. 05	2005.148	21.0	47.39	11	7.8	89	55–131	0.242	10
Mar. 05	2005.221	27.6	47.34	10	3.6	35	16– 60	0.054	70
Apr. 05	2005.283	20.6	47.29	22	7.7	90	52–137	0.053	73
May 05	2005.373	31.6	47.19	18	4.9	43	22– 69	0.079	53
June 05	2005.474	20.6	45.99	19	1.7	19	1– 47	0.227	13
July 05	2005.545	26.7	45.93	14	1.7	16	3– 39	0.048	84
Aug. 05	2005.626	24.0	45.81	19	5.0	52	22– 91	0.118	25
Sep. 05	2005.702	26.0	45.74	19	4.2	40	16– 72	0.081	47
Oct. 05	2005.781	27.0	45.67	12	7.6	80	49–119	0.170	14
Nov. 05	2005.872	30.8	45.57	22	11.7	101	69–140	0.045	77
Dec. 05	2005.953	27.0	45.50	25	12.3	106	74–143	0.089	32
Jan. 06	2006.046	34.8	45.45	13	3.7	32	15– 54	0.102	33
Feb. 06	2006.138	29.7	45.36	30	6.9	71	35–114	0.059	64
Mar. 06	2006.214	24.7	45.27	17	2.2	20	2– 46	0.084	47
Apr. 06	2006.281	23.7	45.22	25	13.6	137	98–182	0.045	78
May 06	2006.370	33.7	45.14	16	6.4	59	33– 92	0.043	83
June 06	2006.461	32.7	45.08	16	5.8	56	33– 86	0.159	16
July 06	2006.546	30.7	45.06	28	7.1	74	34–121	0.108	25
Aug. 06	2006.637	29.7	44.98	21	1.6	18	0– 54	0.129	31
Sep. 06	2006.717	28.7	44.94	20	8.7	91	53–137	0.051	71
Oct. 06	2006.796	28.7	44.89	25	5.7	57	31– 91	0.067	59
Nov. 06	2006.873	23.7	50.88	30	17.0	152	111–199	0.056	65
Dec. 06	2006.948	27.6	50.83	30	6.2	69	31–114	0.056	70
Jan. 07	2007.043	35.6	50.77	25	10.8	89	57–126	0.082	36
Feb. 07	2007.138	30.6	50.66	25	6.8	63	31–103	0.093	36
Mar. 07	2007.214	26.6	50.60	19	4.5	41	19– 70	0.207	7
Apr. 07	2007.279	22.7	50.55	22	2.4	23	3– 50	0.133	28
May 07	2007.368	30.7	50.45	19	7.4	70	38–108	0.069	52
July 07	2007.544	28.7	50.34	21	3.7	36	13– 66	0.044	83
Aug. 07	2007.637	30.8	50.24	22	0.0	0	0– 25	0.068	73
Sep. 07	2007.715	27.5	50.19	24	15.0	130	93–172	0.131	19
Oct. 07	2007.796	29.7	50.13	18	4.7	37	19– 62	0.020	99
Nov. 07	2007.886	29.7	50.02	22	7.9	68	42–100	0.068	55
Dec. 07	2007.964	26.7	49.96	20	8.8	70	44–101	0.043	79

APPENDIX C: MODIFIED CROSS SECTION FOR NEUTRINO CAPTURE

The cross section for neutrino capture by ^{71}Ga was calculated by Bahcall and is given in Table II (best estimate), Table III (3σ lower limit), and Table IV (3σ upper limit) of Ref. [19]. Based on information on the contributions of the excited states given in the text of Bahcall's article, if we assume the matrix element for neutrino capture to the first two excited states of ^{71}Ge to be zero, but that the matrix elements of the other excited states are unchanged, we can approximate the best-estimate cross section in various energy regions as follows:

$$\sigma = \begin{cases} 13.10 + 91.29(E_\nu - 0.24)^{1.157} & \text{for } 0.24 < E_\nu < 0.733 \\ 0.946\,\sigma_{\rm best} & \text{for } 0.733 < E_\nu < 1.033 \\ 0.953\,\sigma_{\rm best} & \text{for } 1.033 < E_\nu < 1.483 \\ 0.96\ \sigma_{\rm best} & \text{for } 1.483 < E_\nu < 1.983 \\ 0.99\ \sigma_{\rm best} & \text{for } 1.983 < E_\nu < 30.0 \end{cases}$$

where $\sigma_{\rm best}$ is the value in Table II of [19], σ is in 10^{-46} cm^2, and the neutrino energy E_ν is in MeV. The results are given in our Table VI. The $\pm 1\sigma$ limits in Table VI were obtained in a similar manner from the 3σ limits given in [19].

TABLE VI: Approximate cross section for neutrino capture by ^{71}Ga if the contribution of the first two excited states is set to zero.

ν energy	Cross section (10^{-46} cm^2)			ν energy	Cross section (10^{-46} cm^2)			ν energy	Cross section (10^{-46} cm^2)		
(MeV)	Best	-1σ	$+1\sigma$	(MeV)	Best	-1σ	$+1\sigma$	(MeV)	Best	-1σ	$+1\sigma$
0.240	1.310E+01	1.280E+01	1.340E+01	1.445	1.944E+02	1.897E+02	2.274E+02	9.500	4.749E+04	4.053E+04	6.275E+04
0.250	1.357E+01	1.326E+01	1.388E+01	1.500	2.153E+02	2.104E+02	2.495E+02	10.000	5.653E+04	4.820E+04	7.474E+04
0.275	1.499E+01	1.465E+01	1.533E+01	1.600	2.451E+02	2.395E+02	2.859E+02	10.500	6.638E+04	5.650E+04	8.785E+04
0.300	1.662E+01	1.624E+01	1.700E+01	1.700	2.771E+02	2.707E+02	3.252E+02	11.000	7.703E+04	6.548E+04	1.020E+05
0.325	1.836E+01	1.794E+01	1.878E+01	1.750	2.939E+02	2.871E+02	3.458E+02	11.500	8.848E+04	7.510E+04	1.173E+05
0.350	2.018E+01	1.972E+01	2.064E+01	2.000	3.932E+02	3.702E+02	4.712E+02	12.000	1.007E+05	8.535E+04	1.336E+05
0.375	2.208E+01	2.157E+01	2.259E+01	2.500	6.428E+02	5.986E+02	7.826E+02	12.500	1.137E+05	9.621E+04	1.508E+05
0.400	2.406E+01	2.351E+01	2.461E+01	3.000	9.806E+02	9.043E+02	1.211E+03	13.000	1.274E+05	1.077E+05	1.692E+05
0.425	2.606E+01	2.546E+01	2.799E+01	3.500	1.449E+03	1.323E+03	1.811E+03	13.500	1.418E+05	1.197E+05	1.884E+05
0.450	2.810E+01	2.746E+01	3.029E+01	4.000	2.108E+03	1.905E+03	2.662E+03	14.000	1.569E+05	1.322E+05	2.086E+05
0.500	3.231E+01	3.157E+01	3.516E+01	4.500	3.043E+03	2.722E+03	3.880E+03	14.500	1.728E+05	1.454E+05	2.298E+05
0.600	4.109E+01	4.015E+01	4.585E+01	5.000	4.336E+03	3.842E+03	5.573E+03	15.000	1.893E+05	1.590E+05	2.520E+05
0.700	5.027E+01	4.912E+01	5.776E+01	5.500	6.072E+03	5.337E+03	7.853E+03	15.500	2.064E+05	1.731E+05	2.749E+05
0.800	6.478E+01	6.329E+01	6.924E+01	6.000	8.350E+03	7.290E+03	1.086E+04	16.000	2.241E+05	1.875E+05	2.988E+05
0.900	7.829E+01	7.649E+01	8.470E+01	6.500	1.133E+04	9.832E+03	1.479E+04	18.000	3.010E+05	2.495E+05	4.025E+05
1.000	9.299E+01	9.085E+01	1.017E+02	7.000	1.515E+04	1.309E+04	1.985E+04	20.000	3.860E+05	3.162E+05	5.184E+05
1.100	1.168E+02	1.142E+02	1.306E+02	7.500	1.989E+04	1.712E+04	2.613E+04	22.500	5.013E+05	4.028E+05	6.778E+05
1.200	1.372E+02	1.341E+02	1.549E+02	8.000	2.550E+04	2.188E+04	3.357E+04	25.000	6.233E+05	4.883E+05	8.501E+05
1.300	1.593E+02	1.557E+02	1.814E+02	8.500	3.198E+04	2.737E+04	4.216E+04	30.000	8.701E+05	6.354E+05	1.217E+06
1.400	1.831E+02	1.789E+02	2.100E+02	9.000	3.928E+04	3.357E+04	5.186E+04				

[1] B. T. Cleveland, T. J. Daily, R. Davis, Jr., J. R. Distel, K. Lande, C. K. Lee, and P. S. Wildenhain, Astrophys. J. **496**, 505 (1998).

[2] J. N. Abdurashitov, V. N. Gavrin, S. V. Girin, V. V. Gorbachev, T. V. Ibragimova, A. V. Kalikhov, N. G. Khairnasov, T. V. Knodel, I. N. Mirmov, A. A. Shikhin, E. P. Veretenkin, V. M. Vermul, V. E. Yants, G. T. Zatsepin, T. J. Bowles, W. A. Teasdale, D. L. Wark, M. L. Cherry, J. S. Nico, B. T. Cleveland, R. Davis, Jr., K. Lande, P. S. Wildenhain, S. R. Elliott, and J. F. Wilkerson, Phys. Rev. C **60**, 055801 (1999) [arXiv.org/abs/astro-ph/9907113].

[3] J. N. Abdurashitov, V. N. Gavrin, S. V. Girin, V. V. Gorbachev, P. P. Gurkina, T. V. Ibragimova, A. V. Kalikhov, N. G. Khairnasov, T. V. Knodel, I. N. Mirmov, A. A. Shikhin, E. P. Veretenkin, V. M. Vermul, V. E. Yants, and G. T. Zatsepin, T. J. Bowles and W. A. Teasdale, J. S. Nico, B. T. Cleveland, S. R. Elliott, and J. F. Wilkerson, Zh. Eksp. Teor. Fiz. **122**, 211 (2002) [J. Exp. Theor. Phys. **95**, 181 (2002)] [arXiv.org/abs/astro-ph/0204245].

[4] J. N. Abdurashitov, V. N. Gavrin, S. V. Girin, V. V. Gorbachev, P. P. Gurkina, T. V. Ibragimova, A. V. Kalikhov, N. G. Khairnasov, T. V. Knodel, V. A. Matveev, I. N. Mirmov, A. A. Shikhin, E. P. Veretenkin, V. M. Vermul, V. E. Yants, G. T. Zatsepin, T. J. Bowles, S. R. Elliott, W. A. Teasdale, B. T. Cleveland, W. C. Haxton, J. F. Wilkerson, J. S. Nico, A. Suzuki, K. Lande, Yu. S. Khomyakov, V. M. Poplavsky, V. V. Popov, O. V. Mishin, A. N. Petrov, B. A. Vasiliev, S. A. Voronov, A. I. Karpenko, V. V. Maltsev, N. N. Oshkanov, A. M. Tuchkov, V. I. Barsanov, A. A. Janelidze, A. V. Korenkova, N. A. Kotelnikov, S. Yu. Markov, V. V. Selin, Z. N. Shakirov, A. A. Zamyatina, S. B. Zlokazov, Phys. Rev. C **73**, 045805 (2006) [arXiv.org/abs/nucl-ex/0512041].

[5] S. Danshin, A. Kopylov, and V. Yants, Nucl. Instrum. Methods Phys. Res. A **349**, 466 (1994).

[6] B. T. Cleveland, Nucl. Instrum. Methods Phys. Res. **214**, 451 (1983).

[7] J. N. Abdurashitov, T. J. Bowles, C. Cattadori, B. T. Cleveland, S. R. Elliott, N. Ferrari, V. N. Gavrin, S. V. Girin, V. V. Gorbachev, P. P. Gurkina, W. Hampel, T. V. Ibragimova, F. Kaether, A. V. Kalikhov, N. G. Khairnasov, T. V. Knodel, I. N. Mirmov, L. Pandola, H. Richter, A. A. Shikhin, W. A. Teasdale, E. P. Veretenkin, V. M. Vermul, J. F. Wilkerson, V. E. Yants, and G. T. Zatsepin, Astropart. Phys. **25**, 349 (2006) [arXiv.org/abs/nucl-ex/0509031].

[8] W. Hampel and L. Remsberg, Phys. Rev. C **31**, 666 (1985).

[9] F. Kaether, Ph. D. thesis, *Datenanalyse der Sonnenneutrinoexperiments Gallex*, Heidelberg, 2007 [www.ub.uni-heidelberg.de/archiv/7501/].

[10] M. Altmann, M. Balata, P. Belli, E. Bellotti, R. Bernabei, E. Burkert, C. Cattadori, R. Cerulli, M. Chiarini, M. Cribier, S. d'Angelo, G. Del Re, K. H. Ebert, F. von Feilitzsch, N. Ferrari, W. Hampel, F. X. Hartmann, E. Henrich, G. Heusser, F. Kaether, J. Kiko, T. Kirsten, T. Lachenmaier, J. Lanfranchi, M. Laubenstein, K. Lützenkirchen, K. Mayer, P. Moegel, D. Motta, S. Nisi, J. Oehm, L. Pandola, F. Petricca, W. Potzel, H. Richter, S. Schoenert, M. Wallenius, M. Wojcik, and L. Zanotti, Phys. Lett. B **616**, 174 (2005) [arXiv.org/abs/hep-ex/0504037].

[11] J. N. Abdurashitov, V. N. Gavrin, S. V. Girin, V. V. Gorbachev, T. V. Ibragimova, A. V. Kalikhov, N. G. Khairnasov, T. V. Knodel, V. N. Kornoukhov, I. N. Mirmov, A. A. Shikhin, E. P. Veretenkin, V. M. Vermul, V. E. Yants, G. T. Zatsepin, Yu. S. Khomyakov, A. V. Zvonarev, T. J. Bowles, J. S. Nico, W. A. Teasdale, D. L. Wark, M. L. Cherry, V. N. Karaulov, V. L. Levitin, V. I. Maev, P. I. Nazarenko, V. S. Shkol'nik, N. V. Skorikov, B. T. Cleveland, T. Daily, R. Davis, Jr., K. Lande, C. K. Lee, P. S. Wildenhain, S. R. Elliott, and J. F. Wilkerson, Phys. Rev. C. **59**, 2246 (1999) [arXiv.org/abs/hep-ph/9803418].

[12] W. C. Haxton, Phys. Rev. C **38**, 2474 (1988).

[13] V. N. Gavrin, A. L. Kochetkov, V. N. Kornoukhov, A. A. Kosarev, and V. E. Yants, Institute for Nuclear Research of the Russian Academy of Sciences Report No. P-777 (1992).

[14] W. Hampel, G. Heusser, J. Kiko, T. Kirsten, M. Laubenstein, E. Pernicka, W. Rau, U. Rönn, C. Schlosser R. v. Ammon, K. H. Ebert, T. Fritsch, D. Heidt, E. Henrich, L. Stieglitz, F. Weirich, M. Balata, F. X. Hartmann, M. Sann, E. Bellotti, C. Cattadori, O. Cremonesi, N. Ferrari, E. Fiorini, L. Zanotti, M. Altmann, F. v. Feilitzsch, R. Mößbauer, G. Berthomieu, E. Schatzmann, I. Carmi, I. Dostrovsky, C. Bacci, P. Belli, R. Bernabei, S. d'Angelo, L. Paoluzi, A. Bevilac-

qua, M. Cribier, I. Gosset, J. Rich, M. Spiro, C. Tao, D. Vignaud, J. Boger, R. L.Hahn, J. K. Rowley, R. W. Stoenner, and J. Weneser, Phys. Lett. **B420**, 114 (1998) [www.mpi-hd.mpg.de/nuastro/gno/restricted/PLB420_98_114.pdf].

[15] W. Hampel, J. Handt, G. Heusser, D. Jaether, J. Kiko, T. Kirsten, M. Laubenstein, E. Neder, E. Pernicka, W. Rau, H. Richter, U. Rönn, U. Schwan, M. Wojcik, Y. Zakharov, R. v. Ammon, K. H. Ebert, T. Fritsch, D. Heidt, E. Henrich, L. Stieglitz, F. Weirich, M. Balata, F. X. Hartmann, E. Bellotti, C. Cattadori, O. Cremonesi, N. Ferrari, E. Fiorini, L. Zanotti, M. Altmann, F. v. Feilitzsch, R. Mößbauer, G. Berthomieu, E. Schatzmann, I. Carmi, I. Dostrovsky, C. Bacci, P. Belli, R. Bernabei, S. d'Angelo, L. Paoluzi, M. Cribier, J. Rich, M. Spiro, C. Tao, D. Vignaud, J. Boger, R. L.Hahn, J. K. Rowley, R. W. Stoenner, and J. Weneser, Phys. Lett. **B436**, 158 (1998) [www.mpi-hd.mpg.de/nuastro/gno/restricted/PLB436_98_158.pdf].

[16] W. C. Haxton, Phys. Lett. B **431**, 110 (1998) [arXiv.org/abs/nucl-th/9804011].

[17] C. Giunti and M. Laveder, Mod. Phys. Lett. A **22**, 2499 (2007) [arXiv.org/abs/hep-ph/0610352].

[18] Y. Farzan, T. Schwetz, and A. Yu Smirnov [arXiv.org/abs/0805.2098].

[19] J. N. Bahcall, Phys. Rev. C **56**, 3391 (1997) [arXiv.org/abs/hep-ph/9710491].

[20] J. N. Bahcall, A. M. Serenelli, and S. Basu, Astrophys. J. Suppl. Ser. **165**, 400 (2006) [arXiv.org/abs/astro-ph/0511337].

[21] C. Peña-Garay, talk at XIIth International Workshop on "Neutrino Telescopes", Venice, 6–9 March 2007. [neutrino.pd.infn.it/conference2007/Talks/PenaGaray.pdf].

[22] N. Grevesse and A. J. Sauval, Space. Sci. Rev. **85**, 161 (1998).

[23] M. Asplund, N. Grevesse, and A. J. Sauval, in ASP Conf. Ser. 336, *Cosmic Abundances as Records of Stellar Evolution and Nucleosynthesis*, ed. by T. G. Barnes III and F. N. Bash, Astro. Soc. Pac., San Francisco, 2005, pp. 25. [arXiv.org/abs/astro-ph/0410214].

[24] F. Confortola, D. Bemmerer, H. Costantini, A. Formicola, Gy. Gyrky, P. Bezzon, R. Bonetti, C. Broggini, P. Corvisiero, Z. Elekes, Zs. Flp, G. Gervino, A. Guglielmetti, C. Gustavino, G. Imbriani, M. Junker, M. Laubenstein, A. Lemut, B. Limata, V. Lozza, M. Marta, R. Menegazzo, P. Prati, V. Roca, C. Rolfs, C. Rossi Alvarez, E. Somorjai, O. Straniero, F. Strieder, F. Terrasi, and H.P. Trautvetter, Phys. Rev. C **75**, 065803 (2007) [arXiv.org/abs/0705.2151].

[25] S. P. Mikheev and A. Yu. Smirnov, Yad. Fiz. **42**, 1441 (1985), [Sov. J. Nucl. Phys. **42**, 913 (1985)]; A. Yu. Smirnov, 10th Int. Workshop on Neutrino Telescopes, Venice, 11-14 March 2003 [arXiv.org/abs/hep-ph/0305106].

[26] S. Abe, *et al.* (KamLAND collaboration), Phys. Rev. Lett. **100**, 221803 (2008) [arXiv.org/abs/0801.4589].

[27] M. C. Gonzalez-Garcia and M. Maltoni, Physics Reports **460**, 1 (2008) [arXiv.org/abs/0704.1800].

[28] V. Barger, D. Marfatia, and K. Whisnant, Physics Letters B **617**, 78 (2005) [arXiv.org/abs/hep-ph/0501247].

[29] J. N. Bahcall, E. Lisi, D. E. Alburger, L. de Braeckeleer, S. J. Freedman, and J. Napolitano, Phys. Rev. C **54**, 411 (1996) [arXiv.org/abs/nucl-th/9601044].

[30] J. N. Bahcall web site www.sns.ias.edu/~jnb.

[31] C. Arpesella, *et al.* (Borexino collaboration) [arXiv.org/abs/0805.3843].

[32] B. Aharmim, *et al.* (SNO collaboration) [arXiv.org/abs/0806.0989].

[33] V. N. Gavrin (SAGE collaboration), Proc. of Eighth Int. Workshop on Topics in Astroparticle and Underground Physics, Seattle, WA, USA, 5–9 September 2003, ed. by F. Avignone and W. Haxton, Nucl. Phys. B (Proc. Suppl.) **138**, 87 (2005).

[34] V. N. Gavrin and B. T. Cleveland, talk at XXII Int. Conf. on Neutrino Physics and Astrophysics, Santa Fe, NM, USA, 13–19 June 2006 [arXiv.org/abs/nucl-ex/0703012].

[35] J. N. Bahcall and C. Peña-Garay, Jour. High Energy Phys. **11**, 004 (2003) [arXiv.org/abs/hep-ph/0305159].

[36] B. T. Cleveland, Nucl. Instrum. Methods Phys. Res. A **416**, 405 (1998).

[37] W. H. Press, S. A. Teukolsky, W. T. Vetterling, and B. P. Flannery, *Numerical Recipes in Fortran*, Cambridge University Press, Cambridge, England, 1992, Section 13.8 [www.nrbook.com/a/bookfpdf/f13-8.pdf].

[38] D. Krofcheck, E. Sugarbaker, J. Rapaport, D. Wang, J. N. Bahcall, R. C. Byrd, C. C. Foster, C. D. Goodman, I. J. Van Heerden, C. Gaarde, J. S. Larsen, D. J. Horen, and T. N. Taddeucci, Phys. Rev. Lett. **55**, 1051 (1985).

[39] H. Ejiri, H. Akimune, Y. Arimoto, I. Daito, H. Fujimura, Y. Fujita, M. Fujiwara, K. Fushimi, M. B. Greenfield, M. N. Harakeh, F. Ihara, T. Inomata, K. Ishibashi, J. Jänecke, H. Kohri, S. Nakayama, C. Samanta, A. Tamii, M. Tanaka, H. Toyokawa, and M. Yosoi, Phys. Lett. B **433**, 257 (1998).

[40] H. Ejiri, Physics Reports **338**, 265 (2000).

[41] R. G. T. Zegers, T. Adachi, H. Akimune, S. M. Austin, A. M. van den Berg, B. A. Brown, Y. Fujita, M. Fujiwara, S. Gales, C.J. Guess, M. N. Harakeh, H. Hashimoto, K. Hatanaka, R. Hayami, G. W. Hitt, M. E. Howard, M. Itoh, T. Kawabata, K. Kawase, M. Kinoshita, M. Matsubara, K. Nakanishi, S. Nakayama, S. Okumura, T. Ohta, Y. Sakemi, Y. Shimbara, Y. Shimizu, C. Scholl, C. Simenel, Y. Tameshige, A. Tamii, M. Uchida, T. Yamagata, and M. Yosoi, Phys. Rev. Lett. **99**, 202501 (2007) [arXiv.org/abs/0707.2840].